Vol 16 No 1, January 2007
1009-1963/2007/16(01)/0228-08
Chinese Physics
© 2007 Chin. Phys. Soc.
and IOP Publishing Ltd

# Discrete gap breathers in a diatomic $K_2$–$K_3$–$K_4$ chain with cubic nonlinearity*

Tian Qiang(田 强)[a)†] and Li Mi-Shan(李宓善)[b)]

[a)] *Department of Physics, Beijing Normal University, Beijing* 100875, *China*

[b)] *Department of Physics, Beijing Jiaotong University, Beijing* 100044, *China*

(Received 23 December 2005; revised manuscript received 17 August 2006)

The discrete gap breathers (DGBs) in a one-dimensional diatomic chain with $K_2$–$K_3$–$K_4$ potential are analysed. Using the local anharmonicity approximation, the analytical investigation has been implemented. The dependence of the central amplitude of the discrete gap breathers on the breather frequency and the localization parameter are calculated. With increasing breather frequency, the DGB amplitudes decrease. As a function of the localization parameter, the central amplitude exhibits bistability, corresponding to the two branches of the curve $\omega = \omega(\zeta)$. With a nonzero cubic term, the HS mode of DGB profiles becomes weaker. With increasing $K_3$, the HS mode of DGB profiles becomes weaker and a bit narrower. For the LS mode, with increasing $K_3$, the central particle amplitude becomes larger, and the DGB profile becomes much sharper. But, as $k_3$ increases further, the central particle amplitude of the LS mode becomes smaller.

**Keywords:** discrete gap breather, diatomic chain, cubic nonlinearity
**PACC:** 6320R, 6320P, 0547

## 1. Introduction

The localized nonlinear time-periodic solutions can exist in pure discrete systems. These localized excitations—discrete breathers (DBs)—were studied in different discrete systems recently.[1−4] Aside from defect-induced localized modes, it has been found that the DBs related to the anharmonicity of the potential can exist in the perfect lattice. These modes are called intrinsic localized modes (ILM)[5] to distinguish them from the defect-localized modes. Over recent decades there has been substantial and increasing interest in the study of DBs in the nonlinear diatomic chain due to the experimental generation and observation in chemical compounds,[6] antiferromagnets,[7] and coupled arrays of Josephson junctions.[8,9]

Both analytical[10,11] and computer-simulation studies[12−16] demonstrated that strongly localized anharmonic modes can occur in a perfect one- or two-dimensional lattice when a quartic term is added to the harmonic potential to characterize the nearest-neighbour restoring force between particles. In a one-dimensional monatomic chain with both positive quadratic and quartic nearest-neighbour interaction potential ($K_2$–$K_4$), the rotating-wave approximation (RWA) has been used to generate intrinsic localized modes above the top of the plane-wave spectrum.[10−12] The original theoretical study on one-dimensional chains with quartic anharmonicity, carried out by Sievers and Takeno,[10] showed the existence of odd-parity localized modes. Subsequent work of Page[11] established the existence of even-parity modes. These modes have frequencies above the maximum harmonic frequency. Bickham *et al*[17] have treated the problem of cubic and quartic anharmonicity showing that there are regions in the ($K_3$, $K_4$) plane where the ILM are stable. In that work they introduced static displacements and used RWA to obtain analytical solutions for even and odd ILM. When a cubic term is added to the interatomic potential ($K_2$–$K_3$–$K_4$ potential), with increasing amplitude, the frequency of a stationary local mode decreases until it approaches the cutoff plane-wave frequency, where the mode becomes unstable.[17]

In a diatomic chain, strongly localized anharmonic modes can occur when a quartic term is added to the harmonic potential to characterize the nearest-neighbour restoring force between particles,[1−3,18] and the localized modes are different from those of the monatomic chain. The linear spectrum of one-dimensional diatomic chain consists of two finite

*Project supported by the National Natural Science Foundation of China (Grant No 10574011).
†Corresponding author: E-mail: qtian@bnu.edu.cn

bands, outside which stable DBs are expected to exist. Franchini *et al*[19] considered a finite number of particles interacting with nearest-neighbour harmonic and cubic and quartic anharmonic potential ($K_2$–$K_3$–$K_4$ potential). They presented some localized modes with frequencies above the top of the optical branch and in the gap between the acoustic and the optical branches. Kiselev *et al*[20,21] introduced the RWA and gave a set of recursion relations for $K_2$–$K_3$–$K_4$ potential. Solving the recursion relations, they obtained the amplitude eigenvector and frequency of localized modes in the gap. Their findings indicated that the experimental search for anharmonic localized modes in real crystals should be directed toward those lattice systems which have a large gap between the optical and acoustic phonon branches. Here we study only the breathers in $K_2$–$K_3$–$K_4$ diatomic chain with frequency inside the gap separating the acoustic and optical bands. These nonlinear localized modes are referred to as discrete gap breathers (DGBs).

The present paper focuses on the characteristics of DGBs in the $K_2$–$K_3$–$K_4$ nonlinear diatomic chain. In addition to the quadratic and quartic nearest-neighbour interaction potential, we examine the effects of the cubic $K_3$-term in the interatomic potential. The outline of this paper is as follows. In Section 2, we introduce the model of a one-dimensional $K_2$–$K_3$–$K_4$ nonlinear diatomic chain and briefly describe the properties of linear waves dispersion relation in this model. In Section 3, based on an asymptotics for the DGBs, the frequencies of the localized modes are analysed. In Section 4, according to the procedure of construction of breathers originally developed in Ref.[3], using both the approximation RWA and LAA, we present some DGB profiles. The next section is devoted to the analysis of the effects of the cubic $K_3$ nonlinearity on the DGBs. The conclusions are given in Section 6.

## 2. The model

We consider the standard one-dimensional diatomic chain with periodically distributed atoms of alternating masses $m$ and $M(M > m)$. The potential of interaction between atoms is taken to be $K_2$–$K_3$–$K_4$ potential

$$V(u_s - u_{s-1}) = \frac{K_2}{2}(u_s - u_{s-1})^2 + \frac{K_3}{3}(u_s - u_{s-1})^3 + \frac{K_4}{4}(u_s - u_{s-1})^4, \tag{1}$$

where $u_s$ is the displacement of the $s$th atom from its equilibrium. Thus, the equation of motion for the $s$th atom reads

$$\begin{aligned}\mu[1 + (-1)^s\delta^2]\ddot{u}_s = &-K_2(2u_s - u_{s+1} - u_{s-1}) \\ &- K_3[(u_s - u_{s+1})^2 + (u_s - u_{s-1})^2] \\ &- K_4[(u_s - u_{s+1})^3 + (u_s - u_{s-1})^3],\end{aligned} \tag{2}$$

where $\mu = (M + m)/2$ and $\delta^2 = (M - m)/(M + m)$.

As is known, the dispersion law of the corresponding linearized equation is

$$\omega_\pm^2 = \frac{K_2}{mM}\Big\{(M + m) \pm (M - m) \times \Big[1 + \frac{4mM\cos^2(qa)}{(M - m)^2}\Big]^{1/2}\Big\}, \tag{3}$$

where the sign '$-$' ('$+$') stands for the acoustic (optical) phonon band, $q$ is the wave number, and $a$ the lattice spacing. The boundaries of the spectrum gap are denoted by $\omega_2$ and $\omega_3$, and

$$\omega_2^2 = 2K_2/M, \quad \omega_3^2 = 2K_2/m. \tag{4}$$

We are interested in DGBs of the set of Eq.(2) with frequencies $\omega$ inside the gap of linear wave spectrum $\omega_2 < \omega < \omega_3$.

In general, four possible localized solutions, centred at a light or a heavy particle with symmetric or antisymmetric profile, may be assumed to exist.[3] In the following sections we examine only the symmetric solutions centred at a heavy particle or at a light particle, called each of these patterns HS and LS modes. The antisymmetric solutions can be treated in the same way. In addition to the well-known rotating wave approximation (RWA), we also introduce a local anharmonicity approximation (LAA), where the nonlinearity in the nearest-neighbour coupling is involved only for the central particle of a breather profile, while the rest particles of the chain are assumed to be coupled with harmonic approximation. The LAA is reasonable, because the DBs' dynamics are similar to those of impurity modes.[3]

## 3. Frequencies of DGBs

Since the linear waves at the frequency gap edges (i.e., at $q = \pi/(2a)$, where $\omega = \omega_{2,3}$) become simply standing waves with out-of-phase oscillations in the neighbouring cells given by $u_{2n} = (-1)^n A\cos(\omega t)$ and $u_{2n+1} = (-1)^n B\cos(\omega t)$, one can assume for the DGBs the following asymptotics, as $n \to \pm\infty$,

$$u_{2n} = (-1)^n A\zeta^{|n|}\cos(\omega t), \tag{5a}$$

$$u_{2n+1} = (-1)^n B\zeta^{|n|}\cos(\omega t), \tag{5b}$$

where $0 < \zeta < 1$ is a localization parameter. Inserting the asymptotics into the equations of motion (2) with $K_3 = 0$ and $K_4 = 0$, we obtain the frequencies that depends on the parameter $\zeta$,

$$\omega_{\pm}^2 = \frac{K_2}{mM}[(M+m) \pm (M-m) \times \sqrt{1 + \frac{mM}{(M-m)^2}(2-\zeta-\zeta^{-1})}, \tag{6}$$

where '$-$' ('$+$') stands for the lower (upper) branch of the curve $\omega = \omega(\zeta)$ plotted in Fig.1. As the minimum of $\zeta + \zeta^{-1}$ is 2, we have $\omega_+ < \omega_3$ and $\omega_- > \omega_2$. The frequencies lie inside the gap of linear wave spectrum $\omega_2 < \omega < \omega_3$ – gap breathers. The relation (6) is the 'dispersion law' for the DGBs. In the following section the numerical procedure of finding such DGBs is described in the LAA approach.

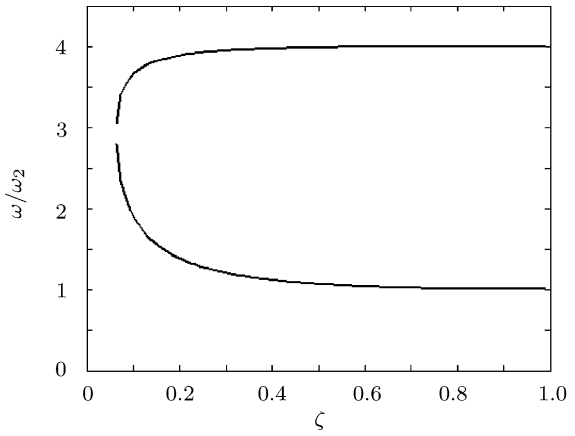



**Fig.1.** Breather frequencies plotted as functions of the localization parameter $\zeta$ with the mass ratio $M/m = 16$ ($\omega_3 = 4\omega_2$).

# 4. Construction of DGBs

DGBs are localized nonlinear time-periodic solutions. The basic property of a DGB is its spatial localization, so that only central particles in DGBs oscillate with large amplitudes. Below we will construct the heavy-particle-centred and light-particle-centred DGBs separately. Using the LAA approach, the nonlinearity in the nearest-neighbour coupling is involved only for the central particle of a breather profile, while the rest particles of the chain are assumed to be coupled with harmonic approximation. We will need to solve the nonlinear equations for the central particle of the breather centred either at a heavy particle or at a light particle, with a symmetric profile (using RWA).

## 4.1. HS mode

For the DGB centred at a heavy particle with symmetric profile (HS mode), e.g., centred at the site with $s = 0$, $u_0$ is supposed to perform large-amplitude oscillations with a certain amplitude $A_0$ and breather frequency $\omega$ ($\omega_2 < \omega < \omega_3$), both of which will be determined from the equations of motion for the central particle and its two adjacent light particles. The other particles are assumed to oscillate symmetrically $u_{-s} = u_s$ with the same frequency $\omega$. In the LAA approach, the equations of motion (2) for the central particle, at the site of $s = 0$, and its nearest-neighbour particles ($s = \pm 1$) become

$$M\ddot{u}_0 = -K_2(2u_0 - u_1 - u_{-1}) - K_3[(u_0-u_1)^2 + (u_0-u_{-1})^2] - K_4[(u_0-u_1)^3 + (u_0-u_{-1})^3], \tag{7a}$$

$$m\ddot{u}_{\pm 1} = -K_2(2u_{\pm 1} - u_{\pm 1+1} - u_{\pm 1-1}) - K_3(u_{\pm 1} - u_0)^2 - K_4(u_{\pm 1} - u_0)^3. \tag{7b}$$

The rest particles of the chain are assumed to be coupled with harmonic approximation.

Accompanying the DGBs asymptotics (5), the HS mode ansatz can entirely be written as follows:[3,22]

$$u_0 = A_0\cos(\omega t), \tag{8a}$$

$$u_{2n} = (-1)^n A\zeta^{|n|}\cos(\omega t), \quad n = \pm 1, \pm 2, \pm 3, \ldots, \tag{8b}$$

$$u_{2n+1} = (-1)^n B\zeta^{n}\cos(\omega t), \quad n = 0, 1, 2, \ldots, \tag{8c}$$

$$u_{2n+1} = (-1)^{n+1} B\zeta^{-(n+1)}\cos(\omega t), \quad n = -1, -2, -3, \ldots. \tag{8d}$$

Schematically, the HS pattern can be represented by the sequence

$$\ldots,$$
$$\zeta^2 B,\ \zeta^2 A,\ -\zeta B,\ -\zeta A,\ B,$$
$$A_0,\ B,\ -\zeta A\ ,-\zeta B,\ \zeta^2 A,\ \zeta^2 B,$$
$$\ldots.$$

Note that $A_0$, $B$ and $A$ are determined from the equations of motion by inserting Eqs.(8) into Eqs.(7). As a result, it is not very difficult to obtain (using RWA)

$$24k_3k_4A_0^3 - 15\Big[3\frac{\omega^2}{\omega_2^2} - 2\Big(\frac{\omega^2}{\omega_3^2} - 1\Big)\frac{1}{\zeta - 1} + 1\Big]k_4A_0^2 + 16\Big[2\frac{\omega^2}{\omega_2^2} + 2\Big(\frac{\omega^2}{\omega_3^2} - 1\Big)\frac{1}{\zeta - 1} - 3\Big]k_3A_0$$

$$-10(\zeta^{-1}+1)=0, \tag{9}$$

where $k_3 = K_3/K_2$ and $k_4 = K_4/K_2$. The amplitude of oscillations of the central heavy particle $A_0$ can be calculated numerically from Eq.(9) for suitable values of the parameters. Then $B$ and $A$ are determined by

$$B=\frac{(\frac{\omega^2}{\omega_2^2}-1)-\frac{4}{5}k_3A_0-\frac{3}{4}k_4A_0^2}{1+\frac{8}{5}k_3A_0+\frac{9}{4}k_4A_0^2}A_0, \tag{10}$$

$$A=\frac{\zeta^{-1}-1}{2(\frac{\omega^2}{\omega_2^2}-1)}B. \tag{11}$$

The amplitudes in each subsequent (more remote from the centre) lateral cell are obtained from the amplitudes in the previous one by multiplying with the factor $-\zeta$. If $k_3 = 0$, it is easy to obtain

$$A_0^2=\frac{2(\zeta^{-1}+1)}{-3k_4[3\frac{\omega^2}{\omega_2^2}-2(\frac{\omega^2}{\omega_3^2}-1)\frac{1}{\zeta^{-1}}+1]}. \tag{12}$$

The expression in the square brackets of Eq.(12) appears to be positive for all the gap frequencies $\omega \in [\omega_2, \omega_3]$, and $0 < \zeta < 1$. This means that the symmetric DGB centred at a heavy particle (HS mode) can exist only if $k_4 = K_4/K_2 < 0$ (soft anharmonicity).

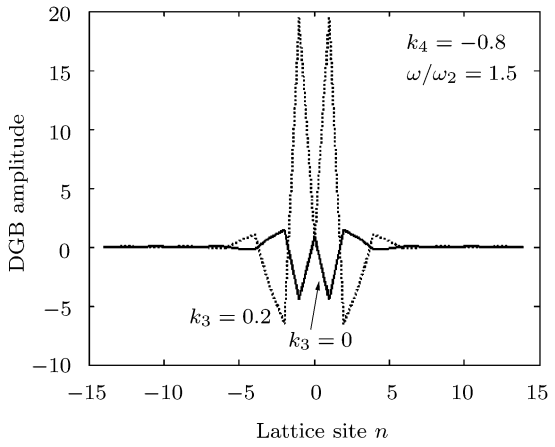



**Fig.2.** The HS pattern for $\omega/\omega_2 = 1.5$ with $k_4 = -0.8$ and $M/m = 16$ ($\omega_3 = 4\omega_2$), plotted for two $k_3$ values ($k_3 = 0$ and 0.2). For $k_3 = 0$, the amplitudes are shown by solid lines, whereas for $k_3 = 0.2$, these are shown by dotted lines.

Thus, the numerical solution for the HS mode as a function of the gap frequency $\omega$ is given by Eqs.(9)–(11). In the case of $k_4 = -0.8$ and $M/m = 16$ ($\omega_3 = 4\omega_2$), the symmetric DGBs centred at a heavy particle with $k_3 = 0$ and 0.2 are illustrated by Fig.2 for the breather frequency $\omega/\omega_2 = 1.5$. The DGBs profiles are sensitive to the nonlinearity of $K_3$. The amplitude of the central heavy particle does not change very much for $k_3 = 0.2$, compared with the case for $k_3 = 0$. But, the amplitudes of its adjacent light and heavy particles become larger for $k_3 = 0.2$ than those for $k_3 = 0$.

## 4.2. LS mode

In the case of the LS mode, the breather is centred at a light particle. We denote the site of the central light particle with $s = 0$ also. In the LAA approach, the equations of motion for the central light particle and its nearest-neighbour particles are

$$\begin{aligned} m\ddot{u}_0 = &-K_2(2u_0-u_1-u_{-1}) \\ &-K_3[(u_0-u_1)^2+(u_0-u_{-1})^2] \\ &-K_4[(u_0-u_1)^3+(u_0-u_{-1})^3], \end{aligned} \tag{13a}$$

$$\begin{aligned} M\ddot{u}_{\pm1} = &-K_2(2u_{\pm1}-u_{\pm1+1}-u_{\pm1-1}) \\ &-K_3(u_{\pm1}-u_0)^2-K_4(u_{\pm1}-u_0)^3. \end{aligned} \tag{13b}$$

The rest particles of the chain are assumed to be coupled in harmonic approximation.

Let $B_0$ be the amplitude of oscillations of the central particle. Equations (5) are reduced to the following ansatz for the LS pattern:

$$u_0 = B_0\cos(\omega t), \tag{14a}$$

$$u_{2n} = (-1)^n B\zeta^{|n|}\cos(\omega t), \quad n = \pm1, \pm2, \pm3, \dots, \tag{14b}$$

$$u_{2n+1} = (-1)^n A\zeta^n\cos(\omega t), \quad n = 0, 1, 2, \dots, \tag{14c}$$

$$u_{2n+1} = (-1)^{n+1} A\zeta^{-(n+1)}\cos(\omega t), \quad n = -1, -2, -3, \dots. \tag{14d}$$

Schematically, the LS pattern of DGBs can be represented by the sequence as follows:

$$\begin{aligned} &\dots, \\ &\zeta^2A,\ \zeta^2B,\ -\zeta A,\ -\zeta B,\ A, \\ &B_0,\ A,\ -\zeta B,\ -\zeta A,\ \zeta^2B,\ \zeta^2A, \\ &\dots. \end{aligned}$$

Similarly, as for the HS mode, the amplitude $B_0$, $A$ and $B$ are determined from the equations of motion by inserting Eqs.(14) into Eqs.(13). We obtain the relations for determining the $B_0$, $A$ and $B$ as follows:

$$24k_3k_4B_0^3-15\Big[3\frac{\omega^2}{\omega_3^2}-2\Big(\frac{\omega^2}{\omega_2^2}-1\Big)\frac{1}{\zeta-1}+1\Big]k_4B_0^2$$

$$+16\Big[2\frac{\omega^2}{\omega_3^2}+2\Big(\frac{\omega^2}{\omega_2^2}-1\Big)\frac{1}{\zeta-1}-3\Big]k_3B_0$$

$$-10(\zeta^{-1}+1)=0, \tag{15}$$

$$A=\frac{\frac{3}{4}k_4B_0^2-\frac{4}{5}k_3B_0+1}{\frac{9}{4}k_4B_0^2-\frac{8}{5}k_3B_0+2(\frac{\omega^2}{\omega_2^2}-1)\frac{1}{\zeta\text{ - }1}}B_0 \tag{16}$$

and

$$B=\frac{2(\omega^2/\omega_2^2-1)}{\zeta-1}A. \tag{17}$$

The numerical solution of the LS mode as a function of the gap frequency $\omega$ is given by Eqs.(15)–(17). Equation (15) determines the amplitude $B_0$ of oscillations of the central light particle for appropriate parameter values. Then, using Eqs.(16) and (17), the amplitude $A$ and $B$ are easily obtained. In the case of $k_4=-0.8$ and $M/m=16$ ($\omega_3=4\omega_2$), the symmetric DGBs centred at a light particle (LS mode) for $k_3=0$ and 0.2 are illustrated by Fig.3 for the breather frequency $\omega/\omega_2=1.5$. With nonzero nonlinearity of $K_3$, the amplitude of the central light particle is larger than that for $k_3=0$.

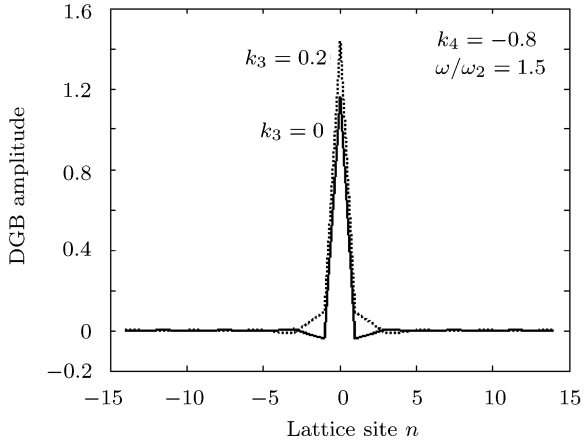



**Fig.3.** The LS pattern for $\omega/\omega_2=1.5$ with $k_4=-0.8$ and $M/m=16$ ($\omega_3=4\omega_2$), plotted for two $k_3$ values ($k_3=0$ and 0.2). For $k_3=0$, the amplitudes are shown by solid lines, whereas for $k_3=0.2$, they are shown by dotted lines.

# 5. Analysis

We here present some further analysis of DGB solutions, especially of the effects of the nonlinearity of $K_3$. For various values of $k_3$, we calculate and analyse the central amplitudes of DGBs as a function of the gap frequency $\omega$ and as a function of localization parameter $\zeta$, and present the DGB profiles with various values of $k_3$.

## 5.1. HS mode

For various values of $k_3$, the dependence of the central amplitude $A_0$ of HS mode on the breather frequency $\omega$ and on the localization parameter $\zeta$ can be calculated by Eq.(9), using the relation (6), and demonstrated in Figs.4 and 5 respectively with $k_4=-0.8$. For $k_3=0$, the central amplitude $A_0$ increases in a region near the acoustic branch in the gap with increasing DGB frequency, and then it decreases. For larger $k_3$ (0.4, 0.6 and 0.8), the central amplitude decreases with increasing DGB frequency, as shown in Fig.4. As a function of the localization parameter $\zeta$, the central amplitude $A_0$ exhibits two values for each $\zeta$, presented in Fig.5. The upper (lower) values correspond to the lower (upper) branch of the curve $\omega=\omega(\zeta)$ (Fig.1).

For a fixed gap frequency $\omega$ which is not near the acoustic branch, the general effect of the cubic anharmonicity is to decrease the central amplitude of the DGBs as $k_3$ increases, as shown in Fig.4 with $\omega/\omega_2=1.5$. As a function of the localization parameter $\zeta$, the central amplitudes $A_0(\zeta)$ are shown in Fig.5 for various values of $k_3$. The two possible amplitudes of $A_0(\zeta)$ correspond to the two branches of the 'dispersion law' $\omega_\pm(\zeta)$ in the relation (6). The larger (small) amplitude of $A_0(\zeta)$ corresponds to the lower (upper) branch of $\omega(\zeta)$.

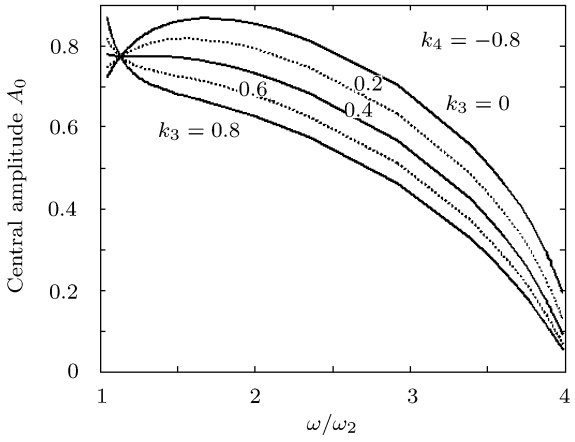



**Fig.4.** The dependence of the central amplitude $A_0$ on the breather frequency $\omega$ with the mass ratio $M/m=16$ ($\omega_3=4\omega_2$) for various values of $k_3$(0, 0.2, 0.4, 0.6 and 0.8).

In Fig.2, we see that the DGB profile with $k_3=0.2$ is larger than that with $k_3=0$. Now, the DGB profiles (HS mode) are shown in Fig.6 for various values of $k_3$(0.2, 0.4, 0.6 and 0.8), with $k_4=-0.8$, $M/m=16$ ($\omega_3=4\omega_2$) and $\omega/\omega_2=1.5$. Notice

that, for nonzero $k_3$, increasing the cubic anharmonicity causes the DGB amplitudes to decrease. And, in the meantime, increasing the cubic anharmonicity does not change the central amplitude very much.

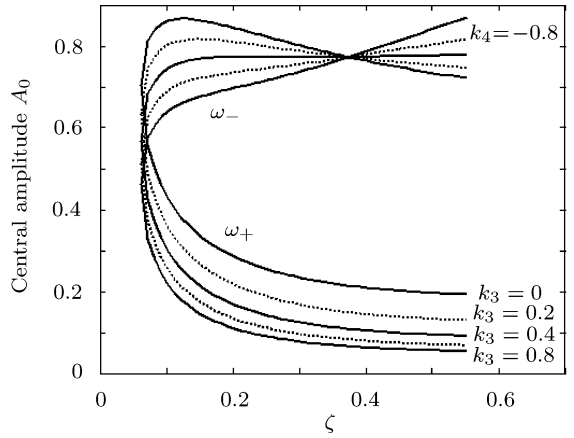



**Fig.5.** The dependence of the central amplitude $A_0$ on the localization parameter $\zeta$ with the mass ratio $M/m = 16$ ($\omega_3 = 4\omega_2$) for various values of $k_3$(0, 0.2, 0.4, 0.6 and 0.8).

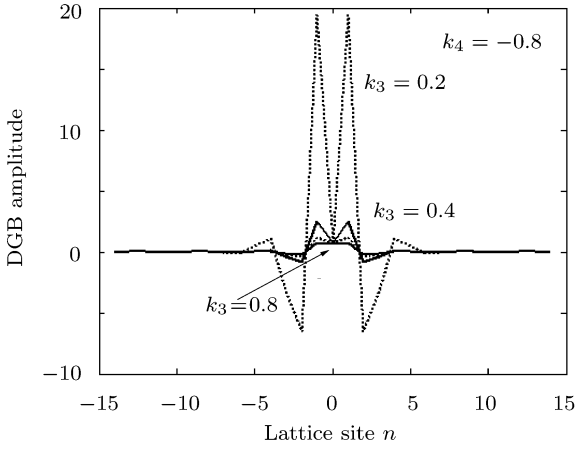



**Fig.6.** The HS mode for $\omega/\omega_2 = 1.5$ with $k_4 = -0.8$ and $M/m = 16$ for various values of $k_3$(0.2, 0.4, 0.6 and 0.8).

## 5.2. LS mode

The dependence of the central amplitude $B_0$ of the LS mode on the breather frequency $\omega$ and on the localization parameter $\zeta$ are calculated for various values of $k_3$ by using Eq.(15), and demonstrated in Figs.7 and 8 separately with $k_4 = -0.8$ and $M/m = 16$ ($\omega_3 = 4\omega_2$). With increasing breather frequency, the central amplitude $B_0$ increases first, and then decreases. As a function of the localization parameter $\zeta$, the central amplitude $B_0$ exhibits two values for each $\zeta$. The upper (lower) values correspond to the lower (upper) branch of the curve $\omega = \omega(\zeta)$ (Fig.1).

For a fixed gap frequency $\omega$, the effect of the cubic anharmonicity $k_3$ on the central amplitude $B_0$ of the HS mode depends on the value of $\omega$, as shown in Fig.7. As a function of the localization parameter $\zeta$, the central amplitudes $B_0(\zeta)$ are shown in Fig.8 for various values of $k_3$. The two possible values of $B_0(\zeta)$ correspond to the two branches of the 'dispersion law' $\omega_\pm(\zeta)$ in Eq.(7). The larger (small) amplitude of $B_0(\zeta)$ corresponds to the lower (upper) branch of $\omega(\zeta)$.

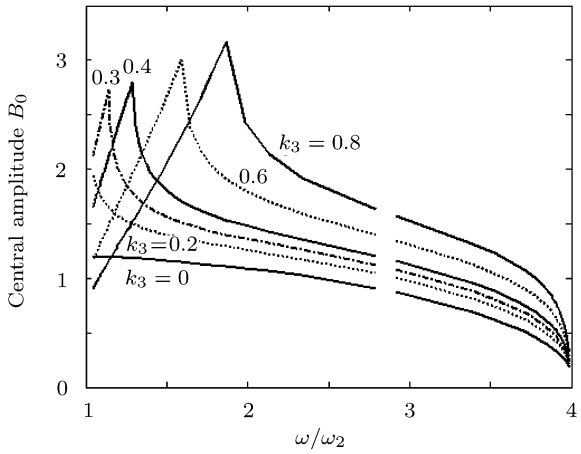



**Fig.7.** The dependence of the central amplitude $B_0$ of LS mode on the breather frequency $\omega$ with the mass ratio $M/m = 16$ ($\omega_3 = 4\omega_2$) for various values of $k_3$(0, 0.2, 0.3, 0.4, 0.6 and 0.8).

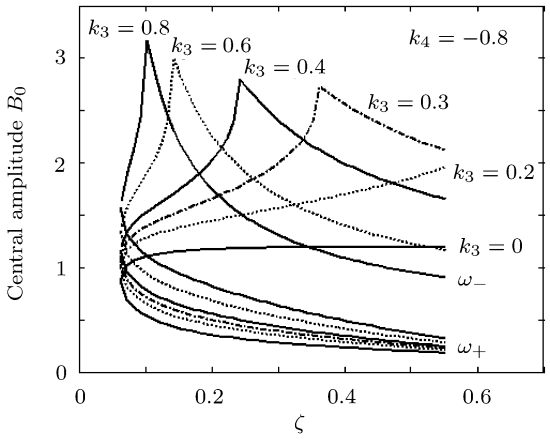



**Fig.8.** The dependence of the central amplitude $B_0$ on the localization parameter $\zeta$ with the mass ratio $M/m = 16$ ($\omega_3 = 4\omega_2$) for various values of $k_3$(0, 0.2, 0.3, 0.4, 0.6 and 0.8).

The DGB profiles (LS mode) for various values of $k_3$(0, 0.2, 0.4, 0.6 and 0.8) are shown in Fig.9 with

$k_4 = -0.8$, $M/m = 16$ for $\omega/\omega_2 = 1.5$. With increasing $k_3$ from 0 to 0.6, the central particle amplitude becomes larger, and the DGB profile becomes more sharper, as shown in Fig.9(a). But, as $k_3$ increases further from 0.6 to 0.8, the central particle amplitude becomes smaller, as shown in Fig.9(b).

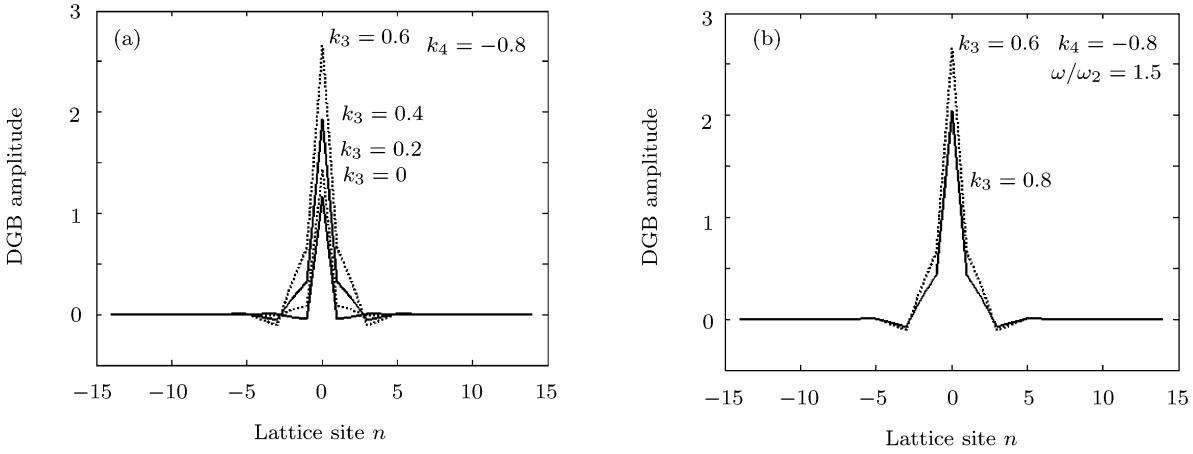



**Fig.9.** The LS mode for $\omega/\omega_2 = 1.5$ with $k_4 = -0.8$ and $M/m = 16$ for various values of $k_3$. (a) $k_3$= 0, 0.2, 0.4 and 0.6 ; (b) $k_3$= 0.6 and 0.8.

## 6. Conclusions

We have investigated the DGBs in a one-dimensional diatomic chain with $K_2$–$K_3$–$K_4$ potential. The $K_2$–$K_3$–$K_4$ potential is more realistic than the one without a cubic term. For a realistic system, the interatomic potential can be expanded about its equilibrium value by using Taylor's theorem. In general, there is a nonzero cubic term in the Taylor expansion. The anharmonic cubic terms are of considerable importance in understanding many physical phenomena.

The analytical investigation of HS mode and LS mode has been implemented, using the RWA and LAA approaches. The antisymmetric solutions can be treated in the same way. We examine the effects of the $K_3$ nonlinearity especially. For various values of $k_3 = K_3/K_2$, we present the dependence of the DGB central-particle amplitude on the breather frequency and on the localization parameter. And, for various values of $k_3$, the DGB profiles are obtained for both HS and LS modes. Cubic anharmonicity plays a central role in the profile of the DGBs. In the case of HS mode, increasing the cubic anharmonicity causes the DGB amplitudes to decrease. In the meantime, increasing the cubic anharmonicity does not change the central amplitude very much.

In the LS mode, the central-particle amplitude becomes larger with increasing $k_3$ and a gap frequency in the lower branch $\omega_-$, and the DGB profile becomes more sharper. But, as $k_3$ increases further, the central particle amplitude becomes smaller. For a gap frequency in the upper branch $\omega_+$, the central-particle amplitude becomes larger with increasing $k_3$.

We expect the investigation and analysis with more realistic potential are useful in understanding of some experimental observations.

## References

[1] Gorbach A V and Johansson M 2004 *Eur. Phys. J.* D **29** 77

[2] Gorbach A V and Johansson M 2003 *Phys. Rev.* E **67** 066608

[3] Maniadis P, Zolotaryuk A V and Tsironis G P 2003 *Phys. Rev.* E **67** 046612

[4] Tian Q and Wang J P 2002 *Int. J. Theor. Phys.* **41**(7) 1275

[5] Kivshar Y S 1991 *Phys. Lett.* A **161** 80

[6] Swanson B I, Brozik J A, Love S P, Strouse G F, Shreve A P, Bishop A R, Wang W Z and Salkola M I 1999 *Phys. Rev. Lett.* **82** 3288

[7] Schwarz U T, English L Q and Sievers A J 1999 *Phys. Rev. Lett.* **83** 223

[8] Trias E, Mazo J J and Orlando T P 2000 *Phys. Rev. Lett.* **84** 741

[9] Binder P, Abraimov D, Ustinov A V, Flach S and Zolotaryuk Y 2000 *Phys. Rev. Lett.* **84** 745

[10] Sievers A J and Takeno S 1988 *Phys. Rev. Lett.* **61** 970
[11] Page J B 1990 *Phys. Rev.* B **41** 7835
[12] Burlakov V M, Kiselev S A and Pyrkov V N 1990 *Solid State Commun.* **74** 327
[13] Bourbonnais R and Maynard R 1990 *Phys. Rev. Lett.* **64** 1397
[14] Burlakov V M, Kiselev S A and Rupasov V I 1990 *Phys. Lett.* A **147** 130
[15] Bickham S R, Sievers A J and Takeno S 1992 *Phys. Rev.* B **45** 10344
[16] Sandusky K W, Page J B and Schmidt K E 1992 *Phys. Rev.* B **46** 6161
[17] Bickham S R, Kiselev S A and Sievers A J 1993 *Phys. Rev.* B **47** 14206
[18] Li M S and Tian Q 2007 *Acta Phys. Sin.* **56**(2) (in print) (in Chinese)
[19] Franchini A, Bortolani V and Wallis R F 1996 *Phys. Rev.* B **53** 5420
[20] Kiselev S A, Bickham S R and Sievers A J 1993 *Phys. Rev.* B **48** 13508
[21] Kiselev S A, Bickham S R and Sievers A J 1994 *Phys. Rev.* B **50** 9135
[22] Zolotaryuk A V, Maniadis P and Tsironis G P 2001 *Physica* B **296** 251